CONF-810732--1

NOTE: This is a draft of a paper being submitted for publication. Contents of this paper should not be quoted nor referred to without permission of the authors.

MASTER

ION-REVERSIBILITY STUDIES IN AMORPHOUS SOLIDS USING THE TWO-ATOM SCATTERING MODEL

Ordean S. Oen

SOLID STATE DIVISION
OAK RIDGE NATIONAL LABORATORY
Operated by
UNION CARBIDE CORPORATION
Under
Contract No. W-7405-eng-26
With the
U. S. DEPARTMENT OF ENERGY
OAK RIDGE, TENNESSEE

June, 1981

MF-01

ION-REVERSIBILITY STUDIES IN AMORPHOUS SOLIDS USING THE TWO-ATOM SCATTERING MODEL*

Ordean S. Oen
Solid State Division, Oak Ridge National Laboratory
Oak Ridge, Tennessee 37830

ABSTRACT

An analytical two-atom scattering model has been developed to treat the recent discovery[1] of the enhancement near 180° of Rutherford backscattering yields from disordered solids. In contrast to conventional calculations of Rutherford backscattering that treat scattering from a single atom only (the backscattering atom), the present model includes the interaction of a second atom lying between the target surface and the backscattering plane. The projectile ion makes a glancing collision with this second atom both before and after it is backscattered. The model predicts an enhancement effect whose physical origin arises from the tolerance of path for those ions whose inward and outward trajectories lie in the vicinity of the critical impact parameter. Results using Molière scattering show how the yield enhancement depends on ion energy, backscattering depth, exit angle, scattering potential, atomic numbers of the projectile and target, and target density. In the model the critical impact parameter and critical angle play important roles. It is shown that these quantities depend on a single dimensionless parameter and analytical expressions for them are given which are accurate to better than 1%.

*Research sponsored by the Division of Materials Sciences, U. S. Department of Energy under contract W-7405-eng-26 with the Union Carbide Corporation.

INTRODUCTION

An unusual enhancement of the yield of low MeV ions backscattered from the near-surface regions of solids for scattering angles very near 180° was reported recently by Pronko, Appleton, Holland and Wilson.[1] The enhancement over that expected for Rutherford scattering occurs at angles a few tenths of a degree from 180° backscattering and increases rapidly as the beam axis is approached. Typically, the enhancement, which may be a factor of two or larger, is a maximum when the ions are backscattered from depths of about 5 to 10 nm. The effect has been observed[1-6] for a wide variety of amorphous and polycrystalline solids using H^+ and He^+ beams of energies from 0.2 to 2.5 MeV.

Barrett[7] suggested that this enhancement effect is a consequence of a correlation between the incoming and outgoing paths of the back-scattered ion, and computer simulation results by Crawford,[8] by Jakas and Baragiola[9] and by Barrett et al.[10] have confirmed this suggestion. In particular the computer simulations of Barrett et al.[10] are in remarkable agreement with the experimental data. Barrett[10] also suggested that the two-atom scattering (blocking) model[11] might shed some insight into this phenomenon.

The purpose of this Communication is to develop and apply the two-atom scattering model[11] to the study of the enhancement of ion backscattering yields from amorphous solids. The model provides a simple physical picture for the origin of the enhancement effect and reproduces its typical features.

BASIC FORMULATION

In conventional Rutherford backscattering calculations[12] applicable to the near surface region of amorphous solids, an ion interacts with a single atom only, the backscattering atom. In the present two-atom model an ion interacts with two atoms: one atom produces the Rutherford backscattering and a second atom back towards the surface scatters the ion both before and after the backscattering event. Classical mechanics is used. Consider a uniform flux intensity I_o of normally incident ions that become backscattered at a depth D in an amorphous target. Let an atom A be located at a distance ℓ above the backscattering plane (see Fig. 1). The particle flux arriving at the backscattering plane will be perturbed by the scattering from atom A. For instance, an incident ion with an impact parameter s will be scattered thru an angle η and arrive at the backscattering plane at a lateral distance $\ell\theta$ from A that is given by

$$\ell\theta = s + \ell\eta \quad , \tag{1}$$

where the small angle approximation is used. Because η, in general, increases with decreasing s, θ has a minimum or critical value θ_c for $s=s_c$ as shown in the top of Fig. 2. (Because of this extremum, backscattered ions need their outgoing trajectories to lie only in the neighborhood of the critical impact parameter, s_c, in order to emerge at angles close to the surface normal. This tolerance of path is the basic reason, in this model, for the enhancement of the backscattering yield). This minimum value of θ produces a shadow or

blocked region behind atom A where no particles can penetrate. The radius of this shadow on the backscattering plane is $\ell\theta_c$. The flux intensity incident on the backscattering plane is easily found from Eq. (1) and is

$$I_i(\theta) = \begin{cases} 0 & \theta < \theta_c \\ I_0 \frac{s}{\ell^2 \theta} \left| \frac{ds}{d\theta} \right| & \theta > \theta_c \end{cases} . \qquad (2)$$

A general feature of $I_i(\theta)$ is that it is highly peaked near θ_c and approaches I_0 for $\theta >> \theta_c$ as illustrated in the bottom of Fig. 2. It is noted that for any given value of θ there are two values of the impact parameter s that contribute to the intensity.

Next consider an isotropic angular distribution of particles starting from atom B that become scattered by atom A before they exit thru the surface (see Fig. 1). The number of particles scattered per unit steradian at angle θ' (θ' is measured with respect to the axis of the dipole BA) is proportional to

$$f(\theta') = \begin{cases} 0 & \theta' < \theta'_c \\ \frac{s'}{\ell^2 \theta'} \left| \frac{ds'}{d\theta'} \right| & \theta' > \theta'_c \end{cases} . \qquad (2a)$$

Here the angle θ' depends on the impact parameter, s', by

$$\ell\theta' = s' + \ell\eta' \quad . \qquad (1a)$$

Since the angles are small the distance between atoms A and B is ℓ. The critical angle θ_c' is found from the extremum of Eq. (1a) which results in a shadow region behind atom A exactly analogous to that discussed following Eq. (1).

Three more factors are important in developing an expression for the backscattered intensity. First, the connection between the incoming and outgoing flux is the Rutherford backscattering event. Since Rutherford scattering changes little over an angular range of a few degrees from 180°, one can simply use the total Rutherford backscattering cross section σ_R for that angular cone. Second, all possible positions of the perturbing atom A relative to the backscattering atom B need to be included. For a random solid the spatial distribution function for finding atom A in a small volume of thickness $\Delta\ell$ is simply $N\ell^2\theta\Delta\ell d\theta d\phi$, where N is the atomic density and ϕ is the azimuthal angle. Third, the two atom model assumes that there is only one significant scattering before the incident particle strikes the backscattering atom. The probability for a single scattering with an impact parameter s is assumed to be $e^{-N\pi s^2 D}$. This exponential factor seems reasonable since it gives the probability that there is no atom in a cylindrical volume of radius s and height D.

Now combining the above three factors with Eqs. (1) and (2), the backscattering intensity per steradian, $I(\psi)$, at small exit angle ψ is

$$I(\psi) = I_o \sigma_R \sum \Delta\ell \iint \frac{s}{\ell^2\theta} \left|\frac{ds}{d\theta}\right| f(\theta') e^{-N\pi s^2 D} N\ell^2\theta d\theta d\phi \quad , \qquad (3)$$

where the summation extends over all atomic layers between the backscattering plane and the surface of the target. The angles θ' and θ are related functionally by $|\theta'| = |\theta - \psi|$ or

$$\theta'^2 = \psi^2 + \theta^2 - 2\psi\theta\cos\phi \ . \tag{4}$$

By changing variables from θ to s Eq. (3) simplifies to

$$\chi(\psi) = \frac{I(\psi)}{I_o \sigma_R} = \sum \frac{\Delta\ell}{D} \int_0^\infty \int_0^{2\pi} f(\theta') e^{-\pi N s^2 D} N D s \, d\phi \, ds \ , \tag{5}$$

where $\chi(\psi)$ is the normalized yield. The above equation is the central result of this paper. In the next section it will be evaluated.

CALCULATIONS

The scattering of the moving ion by the stationary target atom will be described using the Molière interaction potential. In the small angle impulse approximation the scattering angle is

$$n(x) = \frac{b}{a} \{0.6K_1(6x) + 0.66K_1(1.2x) + 0.105K_1(0.3x)\} \ , \tag{6}$$

where x is the ratio of the impact parameter s to the Thomas-Fermi screening distance, $a = 0.04683\ Z_2^{-1/3}$ (nanometers). Here $b = Z_1 Z_2 e^2/E$ where E is the kinetic energy of the ion, $Z_1 e$, $Z_2 e$ are the nuclear charges of the ion and target atom respectively and K_1 is a modified Bessel function of the third kind.

For simplicity it is assumed that the ion loses no energy in backscattering, so that $\theta_c' = \theta_c$. This approximation is very good for

light ions backscattered from heavy targets. The main difficulty in evaluating Eq. (5) arises from the function $f(\theta')$ (Eq. 2a). First, this function is discontinuous and singular at the critical angle, θ_c. Second, it does not seem possible to obtain a closed analytical expression for $f(\theta')$ for scattering from a realistic screened Coulomb potential such as the Molière. Numerical methods, therefore, were used to evaluate Eq. (5). The singularity in $f(\theta')$ is of the form $(\theta'-\theta_c)^{-1/2}$ as may be shown by a Taylor's expansion of θ' about the critical angle. For such singularities Gauss-Mehler quadrature methods are convenient and these were used to evaluate the inner integral over the appropriate ϕ domain. The integral over s was evaluated using a Simpson quadrature technique. The summation in Eq. (5) was done typically by calculating the contribution of 10 atomic layers lying between the surface and the Rutherford backscattering plane.

The three top graphs of Fig. 3 show results of evaluating the double integral of Eq. (5) (omitting the summation) for 1 MeV He ions backscattered from amorphous Pt at a depth of D = 5 nm. Each of the top three graphs shows three distinct regions: an enhancement of the yield at very small ψ, then a deficit region ($\chi < 1.0$), and finally a slight enhancement beginning at $\psi \approx 2\theta_c$. The enhancement at very small ψ is due to backscattered ions whose incoming and outgoing trajectories both pass through the same neighborhood of the critical impact parameter, s_c, of the perturbing atom. For $\psi = 0$ it can be shown that the yield has a logarithmic singularity. The deficit region arises from the blocking or shadowing produced by the perturbing atom on the backscattered ions. The slight enhancement at

$\psi \tilde{>} 2\theta_c$ occurs from ions whose inbound trajectories are near s_c and whose outbound trajectories are near the s_c located on the far side of the perturbing atom. Overall there is particle flux conservation; for instance, if the ordinate is multiplied by sin ψ, it can be shown that the two enhancement regions are exactly compensated by the deficit region. The bottom curve in Fig. 3 is the calculated backscattering yield found by summing over all focussing layers ($\Delta\ell = 0.1D$). It is seen that the enhancement at small ψ is still present, but now the enhancement at larger angles disappears because an enhancement in one layer is cancelled by deficits in other layers.

Equation (5) has been evaluated for several ion-target parameters and results are shown in Figs. 4-9. Figure 4 shows that the yield enhancement is greatest at some intermediate depth and that it is small at both shallow and relatively large depths. In Fig. 5 it is seen that the peak in the normalized yield increases and shifts towards greater depth for decreasing ψ. Figure 6 shows that the yield at $\psi = 0.1°$ increases and peaks at shallower depths with decreasing ion energy. Figure 7 illustrates the yield dependence on the atomic density. Figure 8 shows the influence of the scattering potential on the yield when the screening distance is changed. Shown in Fig. 9 is the yield at $\psi = 0.1°$ for four different target materials. For Al it is seen that the yield is less than unity for depths greater than about 10 nm. This simply means that at those relatively large depths the enhancement is occurring for angles of ψ smaller than 0.1° (this may be inferred from the trend in Fig. 4). Many of the above results may be scaled to other systems by noting that the atomic number and

energy of the ion appear only in the combination $Z_1Z_2e^2/E$. For instance, the same results are predicted for 0.5 MeV protons as for 1.0 MeV alpha particles.

Further insight into the results can be found as follows: the single glancing collision that each ion experiences before being backscattered involves an impact parameter s that is either greater or less than the critical impact parameter s_c. Of those collisions with atoms in an arbitrary focussing plane a fraction $\exp(-\pi Ns^2D)$ involve $s > s_c$, while a fraction $1.0 - \exp(-\pi Ns_c^2D)$ involve $s < s_c$. Now the enhancement effect is expected to be greatest when a maximum number of particles have impact parameters near s_c. This most closely holds when the above two fractions are equal which occurs for $\pi Ns_c^2D = 0.693$. If one takes as a zeroth approximation $s_c^2 \approx b\ell = Z_1Z_2e^2\ell/E$ (Coulomb scattering, see Appendix for Molière scattering) and a focussing plane midway between the surface and the Rutherford plane ($\ell = D/2$), the above equality becomes $\pi NZ_1Z_2e^2D^2 = 1.386\ E$. The predictions of this expression are in qualitative agreement with the enhancement peak shifts in depth found when E or N varied (Figs. 6,7).

Most of the results (Figs. 4-7) of the two-atom model are confirmed by experiment. The main differences are that the model predicts enhancements which are too small and at depths somewhat shallower than found experimentally. As an illustration, predictions of the two-atom model are compared with computer simulation results of Barrett et al.[10] and with experimental measurements[1] in Fig. 10. In this example the model predicts yields which are too little especially

sions in addition to the one included in the two-atom model are contributing to the enhancement effect. It should be mentioned that including the effects of nuclear recoil and depth resolution in the model would lead to poorer agreement.

It has been shown that the two-atom model gives a simple picture of ion path tolerance near the critical impact parameter as the physical origin of the enhancement in the backscattering yield. The model reproduces the typical features of the effect and its dependence on the various physical parameters. It is to date the only analytical model that gives quantitative predictions and an explanation of the enhancement effect. The simplicity and rapidity with which one can do exploratory calculations makes it a complementary approach to the detailed computer simulation methods.

ACKNOWLEDGMENTS

It is a pleasure to acknowledge several fruitful discussions with John Barrett.

APPENDIX

For Coulomb (Rutherford) scattering the function $f(\theta)$ in Eq. (2a) takes on a very simple form[13]

$$f(\theta) = \begin{cases} 0 & \theta < 2\sqrt{b/\ell} \\ \frac{1}{2}\left[\left(1 - \frac{4b}{\ell\theta^2}\right)^{1/2} + \left(1 - \frac{4b}{\ell\theta^2}\right)^{-1/2} \right] & \theta > 2\sqrt{b/\ell} \end{cases} \tag{A-1}$$

where the Coulomb critical angle is $2\sqrt{b/\ell}$. The critical impact parameter for Coulomb scattering is $\sqrt{b/\ell}$. Although these Coulomb expressions are sometimes used in making estimates in discussing blocking phenomena, they are frequently not very accurate. In general, one needs to use a more accurate interaction potential, such as the Molière, that includes the screening of the nuclear charges.

For the Molière potential it does not seem possible to find a closed expression for $f(\theta)$ or even for the critical angle or critical impact parameter. However, as pointed out previously the ratio of the Molière critical angle θ_c to the Coulomb critical angle $2\sqrt{b/\ell}$ is a function of a single parameter $\frac{b\ell}{a^2}$. Although no closed expression for this ratio seems possible, it is found that the following empirical formulas give this ratio to an accuracy of better than 1%.

$$\frac{\theta_c}{2\sqrt{b/\ell}} = \begin{cases} 1.0 - 0.24\sqrt{\alpha} + 0.04\,\alpha & 0 < \alpha < 5 \\ 0.799 - 0.091 \ln\alpha + 0.0016\sqrt{\alpha} & 5 < \alpha < 2500 \end{cases} \tag{A-2}$$

where $\alpha = \frac{b\ell}{a^2}$. Companion expressions that give the ratio of the Molière critical impact parameter s_c to the Coulomb critical impact parameter $\sqrt{b\ell}$ to an accuracy of better than 1% are

$$\frac{s_c}{\sqrt{b\ell}} = \begin{cases} 1.0 & 0 \leq \alpha < 0.1 \\ 1.03 - 0.08\sqrt{\alpha} - 9.6 \times 10^{-5}\,\alpha^2 & 0.1 \leq \alpha < 25 \\ 0.969 - 0.0892 \ln \alpha & 25 \leq \alpha \leq 2500 \end{cases} . \quad \text{(A-3)}$$

As an example of using Eqs. (A-2,3) consider the case $Z_1 = 2$, $Z_2 = 78$, $E = 0.1$ MeV and $\ell = 2.5$ nm. From the formula $a = 0.04683\, Z_2^{-1/3}$(nm) the Thomas-Fermi screening distance is 0.011 nm. Recalling that $e^2 = 1.44$ (eV nm) one finds $\alpha = \frac{b\ell}{a^2} = \frac{Z_1 Z_2 e^2 \ell}{a^2 E} = 46.4$. Using Eq. (A-2) one finds the ratio $\frac{\theta_c}{2\sqrt{b/\ell}} = 0.461$, which shows that the Molière critical angle for this case is less than one-half of that predicted for Coulomb scattering. The Molière critical angle is $\theta_c = 0.0276$ radians or 1.58 degrees. In this example the ratio of the Molière critical impact parameter to the Coulomb critical impact parameter, Eq. (A-3), is $\frac{s_c}{\sqrt{b\ell}} = 0.627$. Here the Molière critical impact parameter is calculated as $s_c = 0.0470$ nm. It is noted that the critical impact parameter is considerably greater than the screening length a = 0.011 nm. It should be mentioned that the universal expressions given in (A-2) and (A-3) also hold when the screening distance is a function of both Z_1 and Z_2 as is true in both the Firsov and Lindhard screening expressions.

The expressions given in Eqs. (A-2) and (A-3) cover a very wide range of ion-target combinations and ion energies since the reduced parameter α ranges from 0 to 2500. The expressions, therefore, are expected to be useful to calculate two-atom critical angles and critical impact parameters which may be used in making estimates in a wide variety of blocking phenomena.[15-19]

REFERENCES

1. P. P. Pronko, B. R. Appleton, O. W. Holland, and S. R. Wilson, Phys. Rev. Lett. 43, 779 (1979).
2. P. P. Pronko, B. R. Appleton, O. W. Holland, and S. R. Wilson, Nucl. Instrum. Methods 170, 227 (1980).
3. B. R. Appleton, O. W. Holland, and J. H. Barrett (to be published in Nucl. Instrum. Methods).
4. R. G. Kirsch and J. C. Poizat, Phys. Lett. 76A, 437 (1980).
5. T. E. Jackman, J. A. Davies, W. Eckstein, and J. A. Moore (to be published in Nucl. Instrum. Methods).
6. J. A. Moore, T. E. Jackman, J. A. Davies, and W. Eckstein (to be published in Nucl. Instrum. Methods).
7. J. H. Barrett, footnote 3 in reference 1 and in reference 2.
8. O. H. Crawford, Phys. Rev. Lett. 44, 185 (1980).
9. M. M. Jakas and R. A. Baragiola, Phys. Rev. Lett. 44, 424 (1980).
10. J. H. Barrett, B. R. Appleton, and O. W. Holland, Phys. Rev. B 22, 4180 (1980).
11. O. S. Oen, Phys. Lett. 19, 358 (1965).
12. Wei-Kan Chu, James W. Mayer, and Marc-A. Nicolet, p. 70 in Backscattering Spectrometry (Academic Press, New York) 1978.
13. J. Lindhard, K. Dan. Vid. Selsk. Mat.-Fys. Medd. 34, No. 14 (1965).
14. O. S. Oen, 7th International Conference on Atomic Collisions in Solids, Moscow, USSR, Sept. 19-23, 1977 (to be published).
15. J. A. Davies, D. P. Jackson, N. Matsunami, P. R. Norton, and J. U. Andersen, Surface Sci. 78, 274 (1978).

16. L. C. Feldman, R. L. Kauffman, P. J. Silverman, R. A. Zuhr, and J. H. Barrett, Phys. Rev. Lett. 39, 38 (1977).

17. J. F. van der Veen, R. M. Tromp, R. G. Smeenk, and F. W. Saris, Nucl. Instrum. Methods 171, 143 (1980).

18. E. S. Mashkova and V. A. Molchanov, Rad. Effests 25, 33 (1975).

19. W. Heiland and E. Taglauer, Surface Sci. 68, 96 (1977).

FIGURE CAPTIONS

Fig. 1. Typical trajecotry of an ion in the two-atom model. The ion makes glancing collisions with atom A before and after being backscattered by atom B. The ion exits the solid at an angle ψ which is measured with respect to the surface normal.

Fig. 2 Top diagram: A plot of Eq. (1) for ℓ = 2nm. Molière scattering, Eq. (6), is used and Z_1 = 2, Z_2 = 78, and E = 1 MeV. Lower diagram: two atom blocking pattern for above case. Curve a corresponds to ions whose impact parameters are less than s_c and curve b to those greater. Curve c is the sum of a and b.

Fig. 3. Top three graphs: Calculated contributions of three selected atomic layers to the backscattering yield for 1 MeV He ions backscattered from amorphous Pt at depth D = 5 nm. It is noted that the point $\psi = 2\theta_c$ depends on ℓ (Eq. 1).

Fig. 4. Calculated backscattering yield vs angle for 1 MeV He ions from different depths in amorphous Pt.

Fig. 5. Calculated ion backscattering yield vs depth for different exit angles ψ for 1 MeV He ions from amorphous Pt.

Fig. 6. Calculated He ion backscattering yield in amorphous Pt vs depth for different ion energies.

Fig. 7. Calculated backscattering yield in Pt for 1 MeV He ions for different atomic densities (the normal density N = 66.4 atoms/nm^3 curve is dashed for clarity).

Fig. 8. Calculated backscattering yield in Pt for 1 MeV He ions for different atomic screening distances (a = 0.011 nm is normal).

Fig. 9. Calculated backscattering yield vs depth for 1 MeV He ions for different amorphous solids.

Fig. 10. Comparison of the two-atom model results with experiment[1] and computer simulations[10] for 1 MeV He ions backscattered from amorphous Pt. The open circles include depth resolution appropriate to the detector used in the experiment.

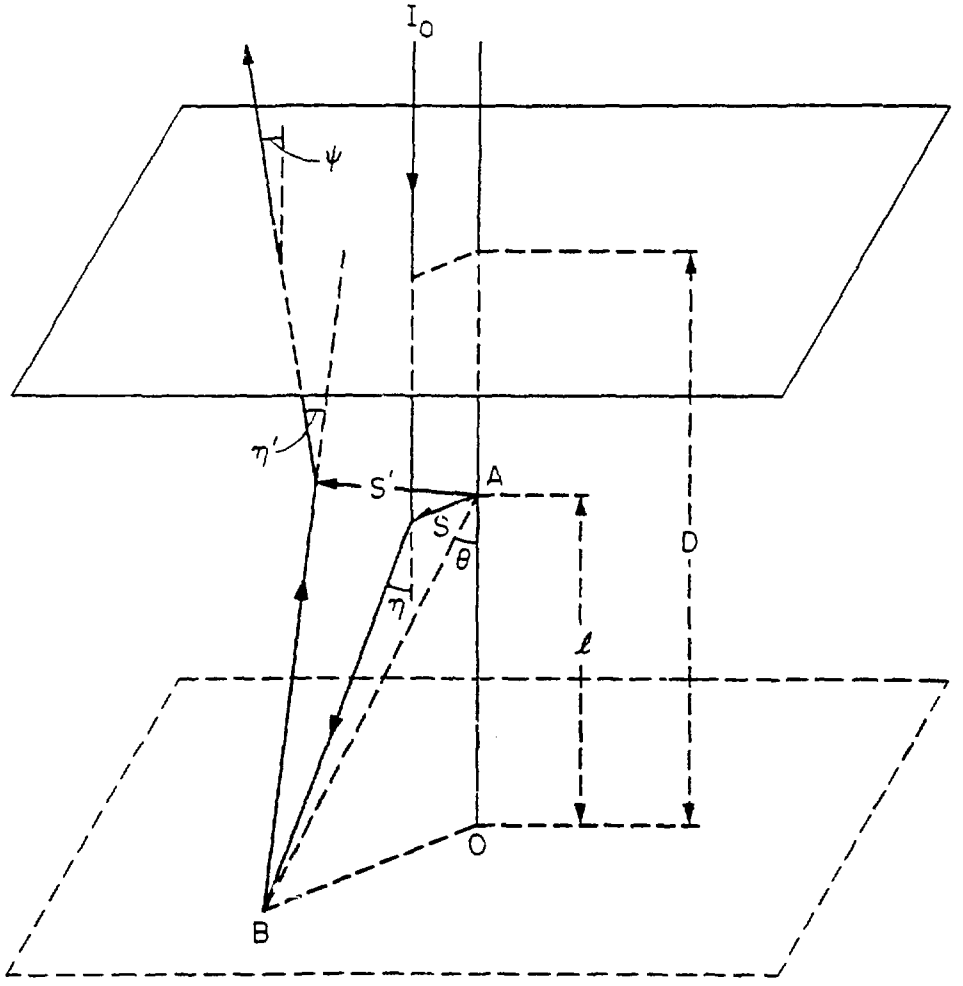

Fig. 1

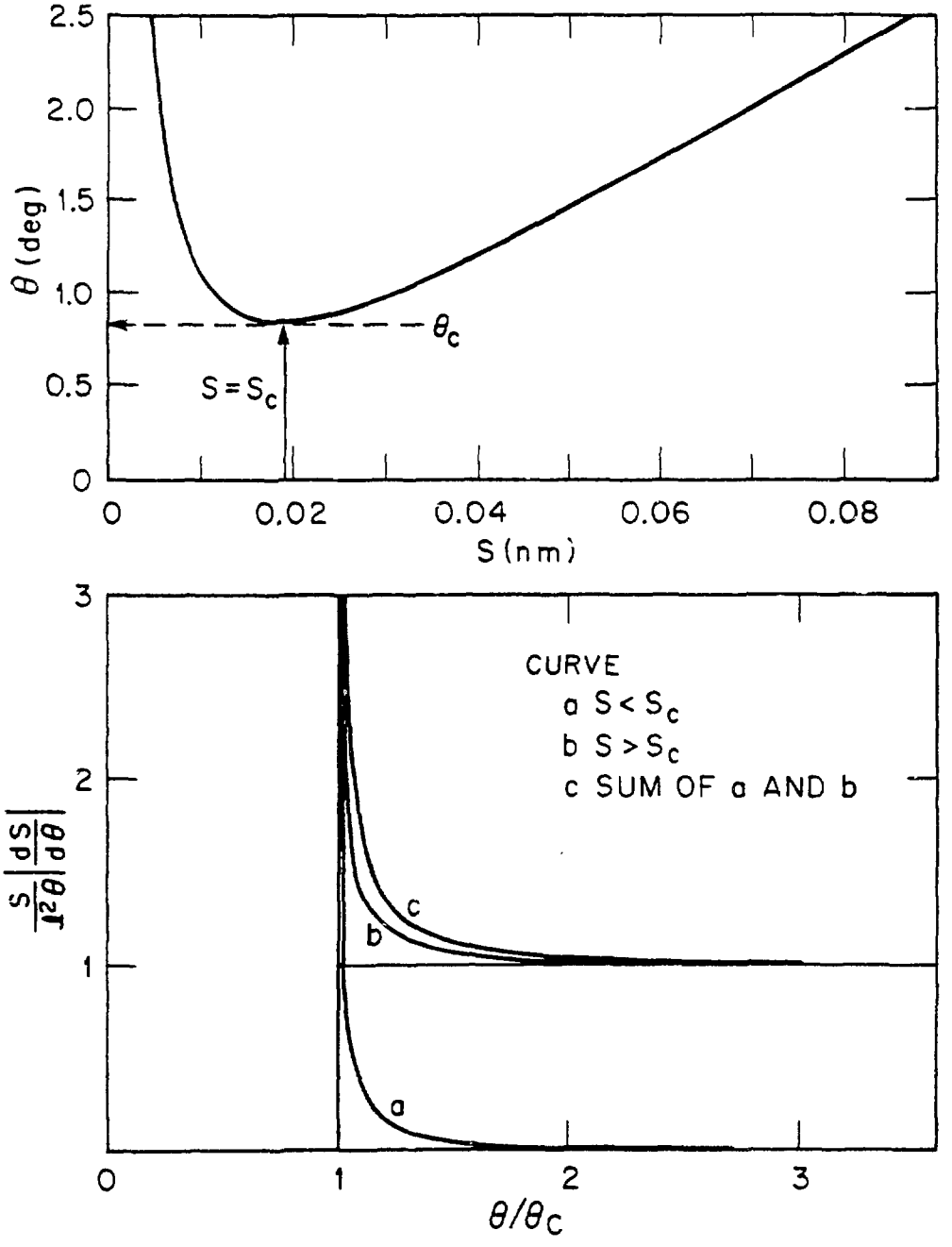
2.5
2.0
1.5
1.0
0.5
0
θ (deg)
θc
S = Sc
0
0.02
0.04
0.06
0.08
S (nm)
3
2
1
0
1
2
3
θ/θc
CURVE
a S < Sc
b S > Sc
c SUM OF a AND b
a
b
c

Fig. 2

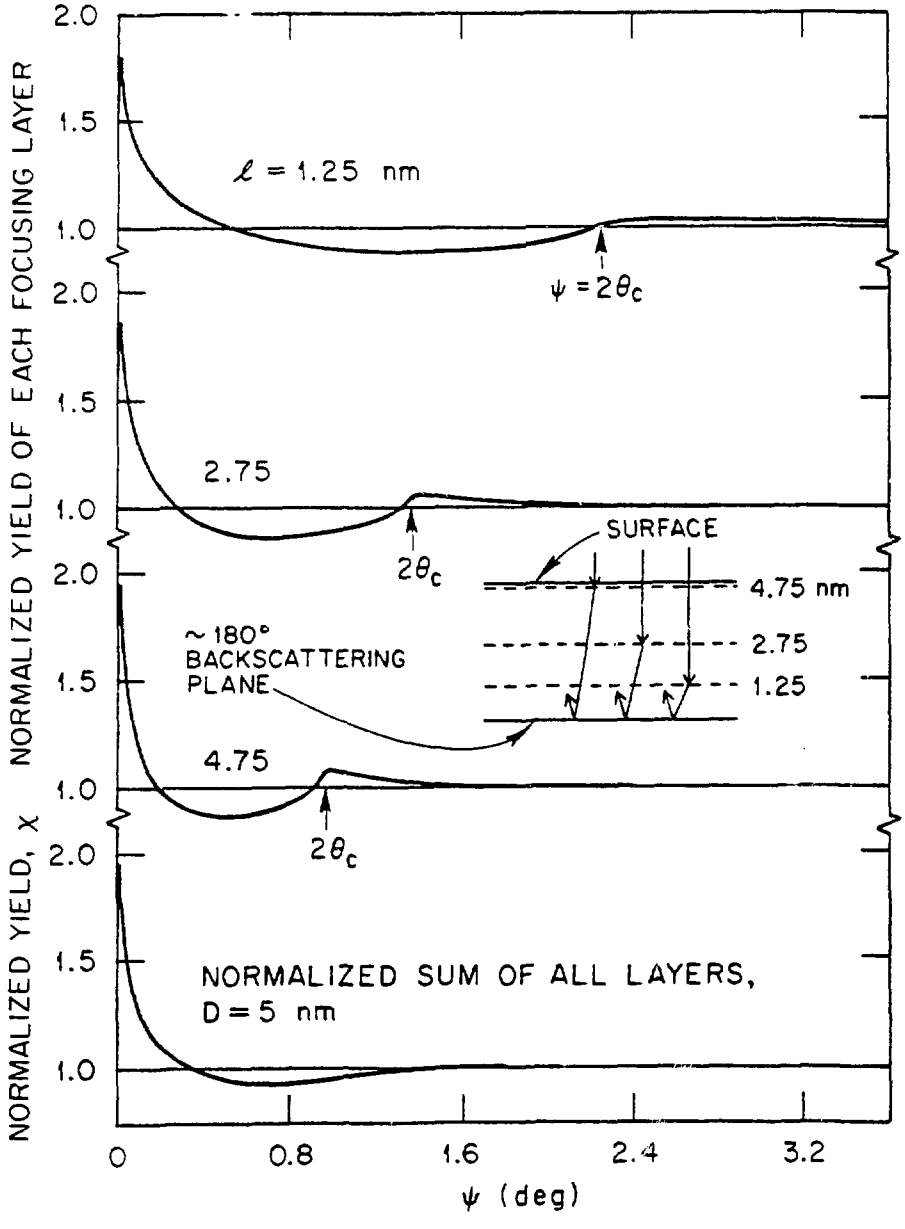
NORMALIZED YIELD OF EACH FOCUSING LAYER
NORMALIZED YIELD, χ
2.0
1.5
1.0
ℓ = 1.25 nm
ψ = 2θc
2.75
2θc
SURFACE
4.75 nm
2.75
1.25
~ 180°
BACKSCATTERING
PLANE
4.75
2θc
NORMALIZED SUM OF ALL LAYERS,
D = 5 nm
0
0.8
1.6
2.4
3.2
ψ (deg)

Fig. 3

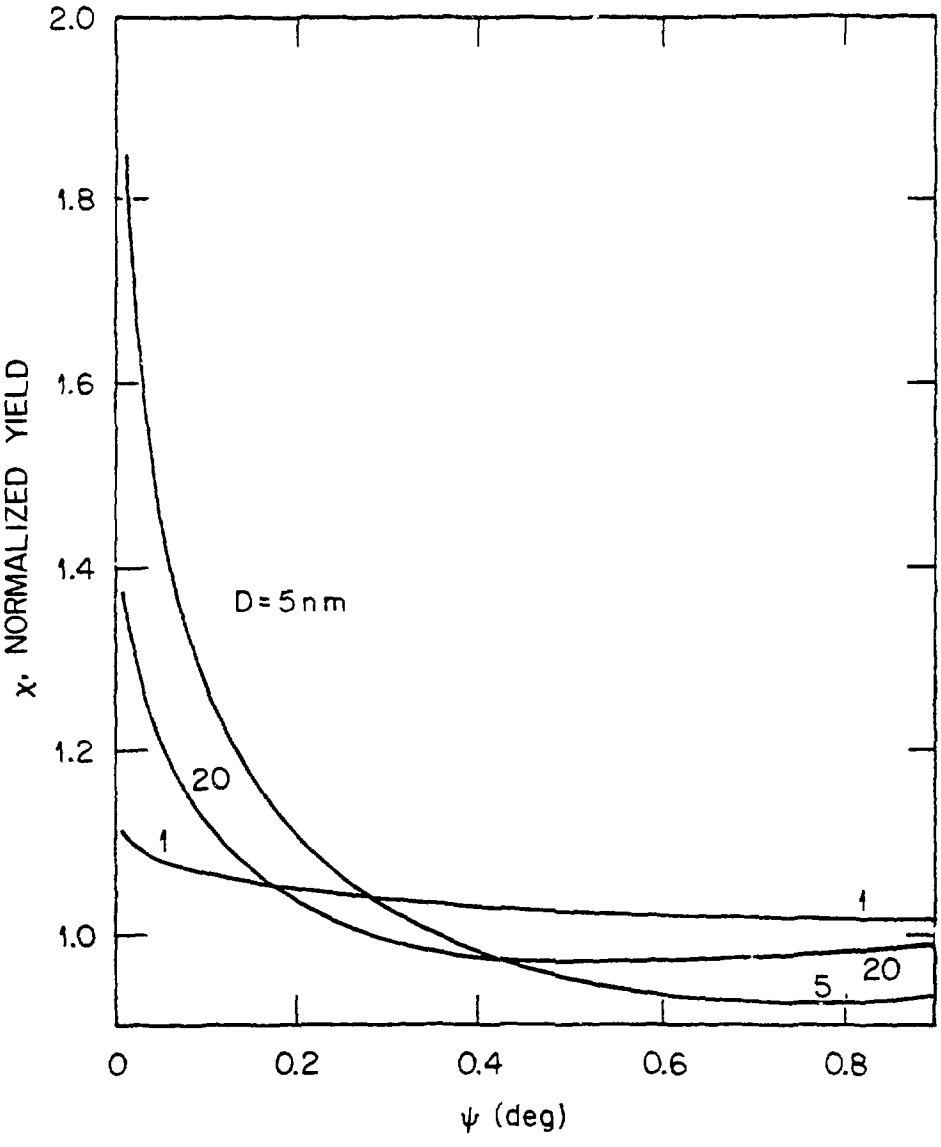
2.0
1.8
1.6
1.4
1.2
1.0
χ, NORMALIZED YIELD
D=5nm
20
1
1
5
20
0
0.2
0.4
0.6
0.8
ψ (deg)

Fig. 4

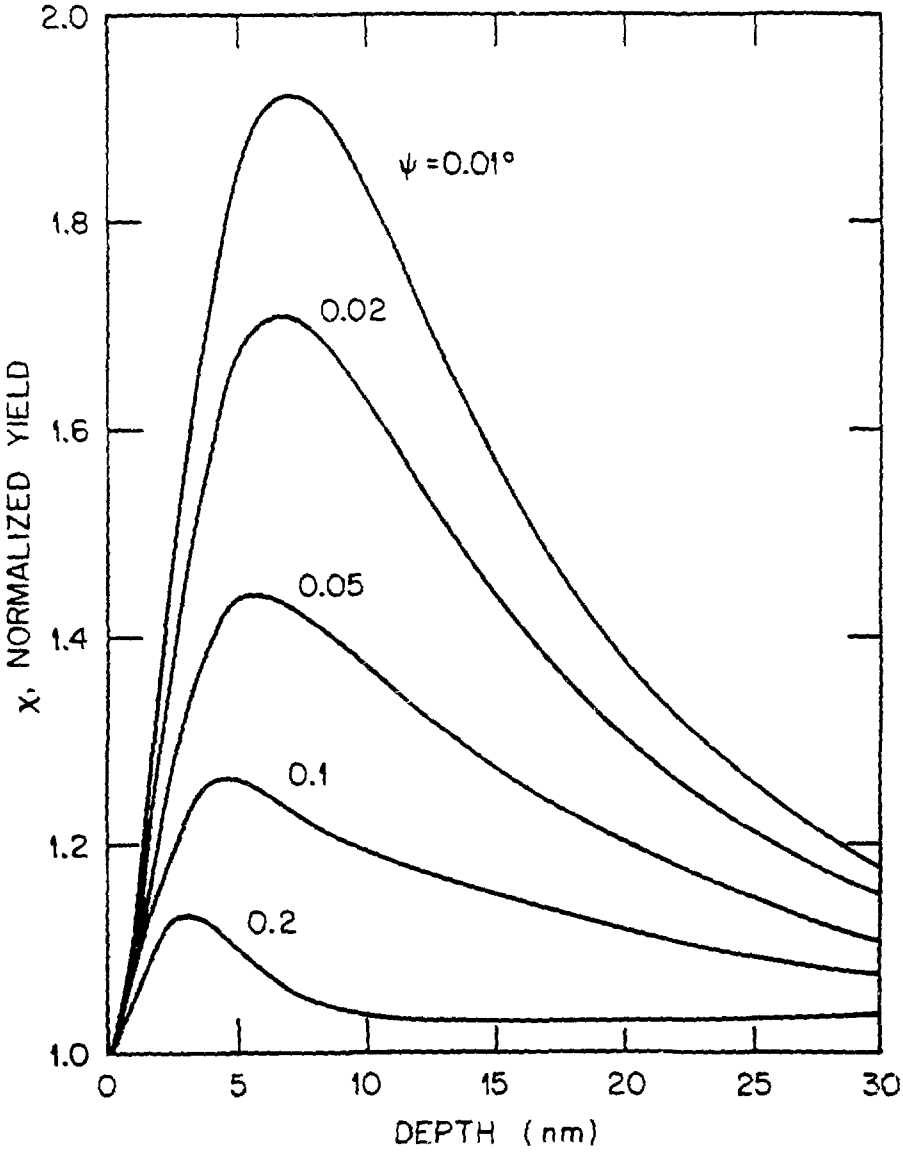
2.0
1.8
1.6
1.4
1.2
1.0
χ, NORMALIZED YIELD
ψ = 0.01°
0.02
0.05
0.1
0.2
0
5
10
15
20
25
30
DEPTH (nm)

Fig. 5

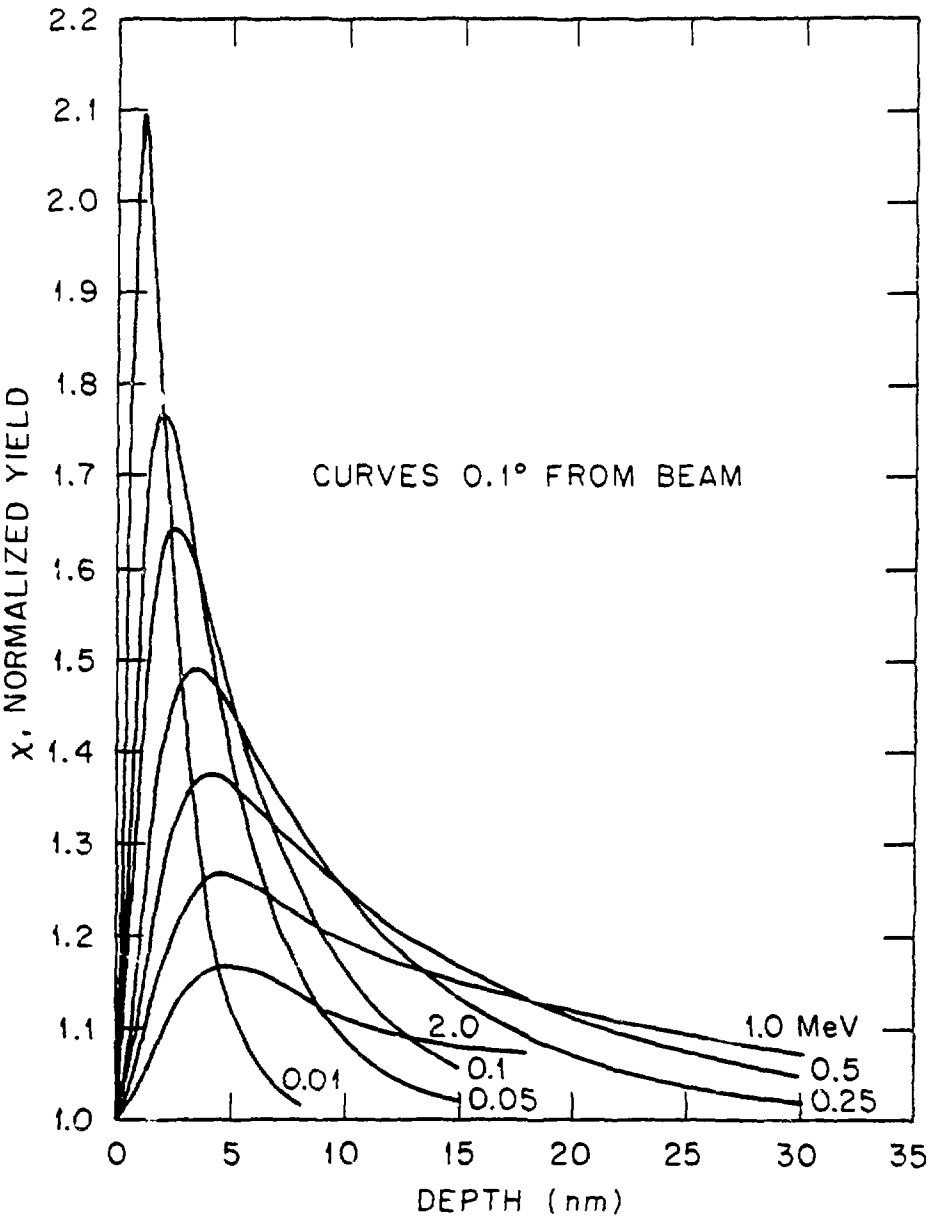
2.2
2.1
2.0
1.9
1.8
1.7
1.6
1.5
1.4
1.3
1.2
1.1
1.0
χ, NORMALIZED YIELD
CURVES 0.1° FROM BEAM
2.0
1.0 MeV
0.1
0.5
0.01
0.05
0.25
0
5
10
15
20
25
30
35
DEPTH (nm)

Fig. 6

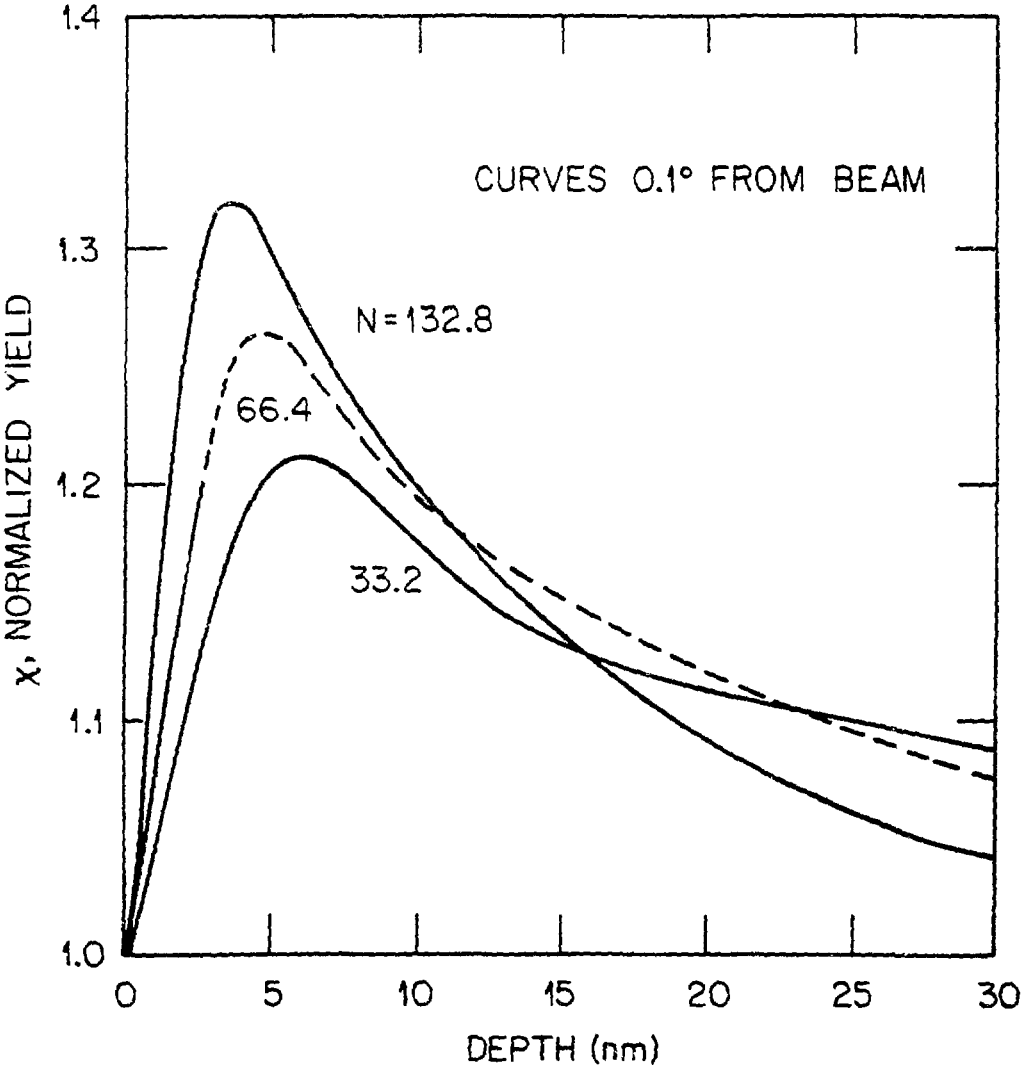
CURVES 0.1° FROM BEAM
N=132.8
66.4
33.2
χ, NORMALIZED YIELD
DEPTH (nm)
1.4
1.3
1.2
1.1
1.0
0
5
10
15
20
25
30

Fig. 7

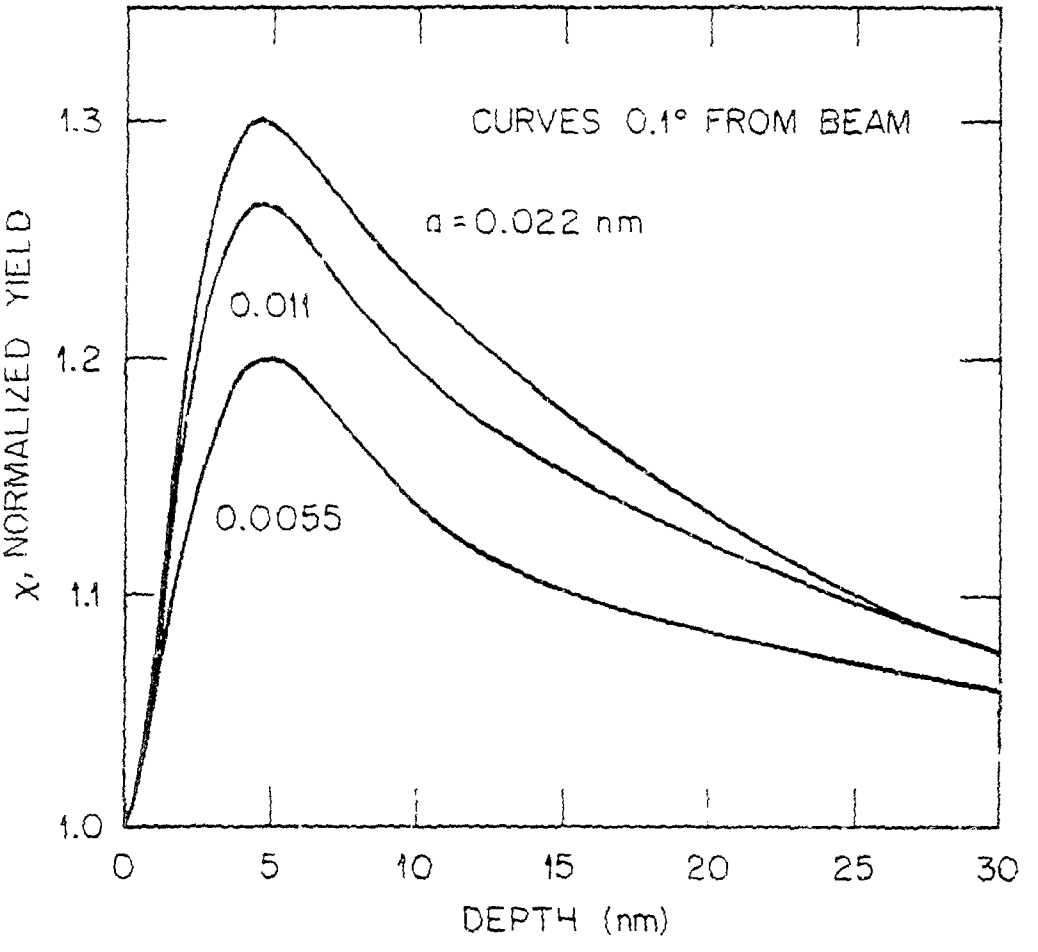
CURVES 0.1° FROM BEAM
a = 0.022 nm
0.011
0.0055
χ, NORMALIZED YIELD
1.3
1.2
1.1
1.0
0
5
10
15
20
25
30
DEPTH (nm)

Fig. 8

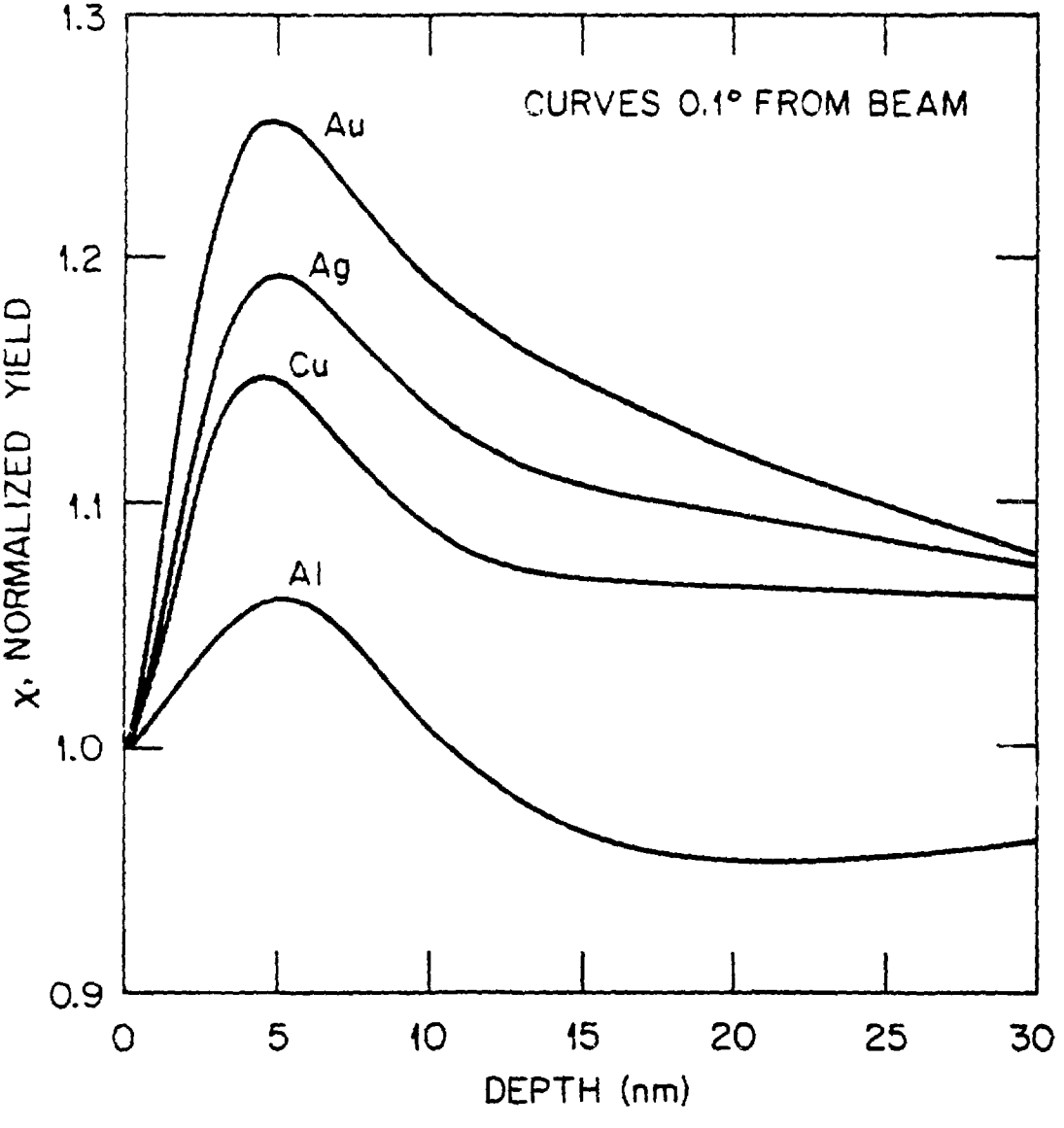
CURVES 0.1° FROM BEAM
Au
Ag
Cu
Al
χ, NORMALIZED YIELD
1.3
1.2
1.1
1.0
0.9
0
5
10
15
20
25
30
DEPTH (nm)

Fig. 9

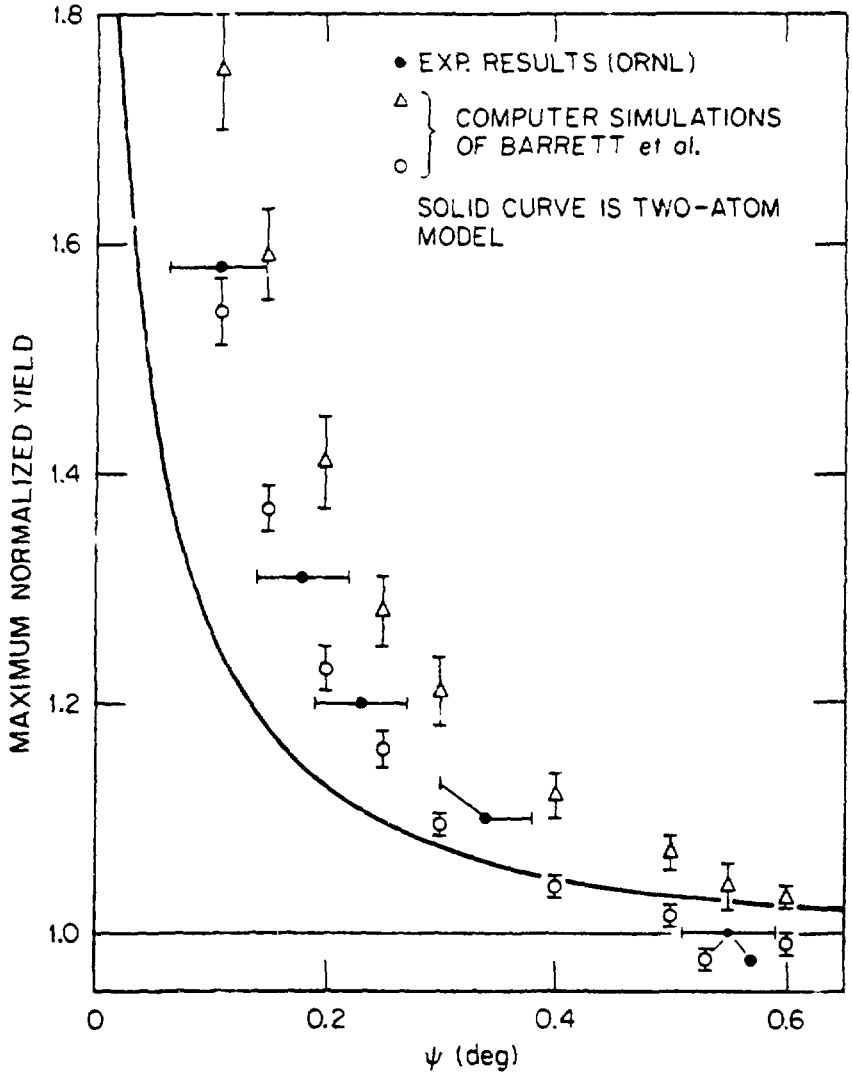
1.8
1.6
1.4
1.2
1.0
MAXIMUM NORMALIZED YIELD
• EXP. RESULTS (ORNL)
△ ○ COMPUTER SIMULATIONS OF BARRETT et al.
SOLID CURVE IS TWO-ATOM MODEL
0
0.2
0.4
0.6
ψ (deg)

Fig. 10